All-Painting Process To Produce Respiration Sensor Using Humidity-Sensitive Nanoparticle Film and Graphite Trace

Kano, Shinya

Fujii, Minoru

All-painting process to produce respiration sensor using humidity-sensitive nanoparticle film and graphite trace

Shinya Kano and Minoru Fujii*

Department of Electrical and Electronic Engineering, Graduate School of Engineering, Kobe University, 1-1, Rokkodai, Nada, Kobe 657-8501, Japan

*Email address: kano@eedept.kobe-u.ac.jp

KEYWORDS

All-painting process, health monitoring, respiration sensor, nanoparticle film, humidity

ABSTRACT

We propose an all-painting process to produce a respiration sensor made from a humidity-sensitive nanoparticle (NP) film and a graphite trace. The sensor is fabricated under ambient air with a simple vacuum-free process for green electronics: solely hand-painting on a cellulose acetate film. A humidity-sensitive silica NP film is painted by brush on pencil-trace graphite electrodes. An all-painted humidity sensor using this film shows 10^6 % sensitivity within a 10-93% humidity change. The film is flexible and the humidity sensor operates as a respiration sensor after bending test. We design an all-painted respiration sensor using the humidity sensor

and a painted resistor. Finally, we integrate the all-painted respiration sensor, a flexible temperature sensor, and a portable data logger as a portable bifunctional healthcare device. The device on a mask can monitor human respiration rate and exhaled air temperature simultaneously.

Importance of healthcare devices has been increasing rapidly in modern life. Health monitoring and fitness tracking of vital signs are demands to use healthcare devices[1–3]. Continuous monitoring of vital signs is helpful for early detection of symptoms and disease. In hospital, vital signs of patients are automatically monitored by a bedside monitor with electrical wires to body. Vital signs during fitness and sports activities are usable to assess performance of exercises. A heart rate monitoring system has already been installed in commercial fitness trackers[4] and the data are collected via wireless communication into smartphones. Recently, monitoring multiple physiological signals by using a single multifunctional device is intensively studied[5–9].

Respiration rate is one of the vital signs and directly relates to the condition of respiratory organs. In order to detect respiration rate remotely, several types of portable respiration sensors have been proposed[10–17]. Colloidal nanomaterial films are promising as a humidity-sensitive film to detect respiration[18,19]. Non-heat resistant polymer films can be in use as a substrate when solution processes to deposit colloidal nanomaterials are carried out at low temperature (< 100 ºC). Paper (cellulose) is an attracting green material as a platform of electrical devices because of low cost, lightweight, environmental friendliness, and availability of printing processes[20–22]. Various electrical devices have been developed on a paper[20]: field-effect transistors[23,24], capacitive touch pads[25], memories[26,27], and sensors[28–33]. On a paper, conductive graphite is easily deposited as a pencil trace. The advantages of graphite trace are light, robust, and stable against chemical corrosion[21]. Electrical circuits on paper are easily drawn and modified as compared to conventional lithography and metal deposition processes. Flexible electrical devices using a pencil trace are reported in recent literatures[28,33–35]. Zhao et al. demonstrated a humidity sensor with drawn graphite and multi-walled carbon nanotube layers.[34] They patterned outlines of graphite interdigitated electrodes by printing with AutoCAD. Zhang et al. draw graphite on Ag-Pd interdigitated electrodes to form a simple

humidity sensor.[35] Kanaparthi showed a pair of graphite electrodes on a paper worked as a capacitive respiration sensor. The sensor on a textile mask monitored human respiration although a numerical derivation of the signal was required to find respiration rates.

Inspired by these works, we propose a simple sensor fabrication process: painting a respiration sensor with a humidity-sensitive nanoparticle (NP) film and graphite trace. All-printed devices are usually fabricated by using inkjet and screen printers[27,36,37]. In this study, we define an "all-painted" sensor fabricated solely by hand-painting. Fabrication of all-painted sensors is simple and vacuum free without any electronic facilities. Low-cost and non-toxic green materials such as silica (SiO_2) NP and graphite are used for this process. For electrical interconnection, we use graphite trace as a contact electrode in this work. A SiO_2 NP film, which is a humidity sensitive film, is painted on the electrodes by a brush with a colloidal NP solution[16,38,39]. A fabricated device works as a humidity sensor. We characterize the humidity-sensing capability and the sensor. We design an all-painted resistor for fabricating a respiration sensor as well. By implementing an all-painted respiration sensor and a flexible thermistor on a mask, a portable bifunctional healthcare device is produced. The healthcare device can observe respiration rate and exhaled air temperature of a subject. The respiration sensor shows clear respiration signals with high signal-to-noise ratio without baseline drifting.

EXPERIMENTAL SECTION

Fabrication of all-painted sensor. The process for the fabrication of a SiO_2 NP sensor by painting is schematically shown in Figure 1(a). As a flexible substrate, we adopted a single-side mending tape (3M, Scotch Magic Tape) based on a cellulose acetate film. The surface of the tape was matte finished and this tape had a write-on capability by a pencil. A cellulose paper such as a photocopying paper also worked as a substrate. However, the response of a sensor on a photocopying paper was much slower than that on a cellulose acetate film as discussed later. Graphite electrodes were deposited on the tape by using a mechanical pencil with a HB pencil lead and a metal mask. The metal mask had patterns of electrodes (5 mm square) and 200 μm spacing. Sheet resistance of graphite electrodes was 50-100 kΩ/sq. and did not change by exposure to respiration. The sheet resistance does not largely affect the sensor output because the resistance of a SiO_2 NP film is much larger as shown later. Zhao et al. reported that the square resistance of graphite electrodes decreased as the graphite content of pencil leads increased.[34] A colloidal solution of SiO_2 NPs (Nissan Chemical Industries Ltd., ST-XS) was deposited by using a brush between the graphite electrodes and dried at room temperature. A deposited solution was kept on a top of the acetate film and a NP film was gradually formed. The whole fabrication processes were carried out under ambient air. It should be noted that a NP film covered with a cellulose acetate tape did not respond to humidity change: thus the surface-covered NP film worked as a resistor.

Figure 1(b) shows a photo of an all-painted film and an optical microscopy image. Although the NP film is cracked, the resistance of the film responds to humidity change as shown later: therefore, the cracked area is also covered with thin NP layers. Figure 1(c)-(e) show atomic force microscopy (AFMWorkshop, TT-2) images of an acetate film, a graphite electrode, and a SiO_2 NP film (un-cracked area). Height gradient curves are also shown in

Figure 1(f). On a graphite electrode, step structures possibly due to graphite flakes are observed (Figure 1(d)). Surface of a SiO_2 NP film is flatter than that of a bare acetate film, which indicates that NPs are densely packed[40]. The thickness of the NP film is approximately 400 nm from line profiles in Figure S1. The scanning electron microscope image of a NP film and a graphite electrode is shown in Figure S1(d). Fabricated all-painted sensors on a 25 μm-thick polyimide film are flexible and can be wrapped around a pen with 8 mm diameter as shown in Figure 1(g).

Measurement setup. The humidity-sensing property of an all-painted sensor was measured in a homemade box or a closed vessel with saturated salt solutions. Relative humidity (RH) in the box was controlled by N_2 carrier gas with bubbling distilled water. In case of a closed vessel with saturated salt, relative humidity conditions of 33, 67, 84, 93 %RH were obtained by using saturated solutions of $MgCl_2$, $CuCl_2$, KCl, and KNO_3, respectively. Current through the film was measured by a source measure unit (Keithley, 236). RH in the box was simultaneously recorded by using a commercial humidity sensor (TDK, CHS-UGS). The accuracy of the commercial sensor was ± 5 % of RH. Impedance spectroscopy was carried out by using an LCR meter (NF Corporation, ZM2376). Frequency of AC voltage was changed from 1 Hz to 1 MHz.

For evaluating dynamic response of resistance of SiO_2 NP films, we used a saturated KCl solution in a closed vessel which had 84 % RH[41,42]. We monitored resistance of the films while taking the sensor into and out of the vessel. The measurements were carried out in room temperature and 30 % RH. We evaluated response and recovery time by observing current intensity to humidity change. Bending tests of painted sensors were carried out by using a Vernier caliper. Radius of curvature (r) was changed from 10 to 1.3 mm. We made bending cycle tests up to 500 times.

Fabrication of bifunctional healthcare device. We integrate an all-painted respiration sensor, a flexible thermistor (SEMITEC, 103JT-025-A; resistance of thermistor R_T = 9.67 kΩ; response time ~5 s), and a portable data logger (MbientLab, MetaWearC) into a portable bifunctional healthcare device. A load resistor for reading a voltage change was also painted by using the method in Figure 1(a). We introduced a thermistor to estimate exhaled air temperature and a temperature in air (when no exhaled air is given). Evaluation of exhaled air temperature has been suggested as a non-invasive method in human physiology and clinical researches.[43] We made the devices electrically contacted with a silver epoxy paste and a polyurethane wire. The devices were mounted on a 125-μm thick polyimide film for stable measurements. The healthcare device was attached on a medical oxygen mask with a single-side tape. The subject wearing the device recorded their respiration rate and exhaled air temperature simultaneously. The data were collected by using an Android API for MetaWearC in a tablet under 26-28 ºC. Respiration rate was calculated by counting the number of respiration in every 30 s.

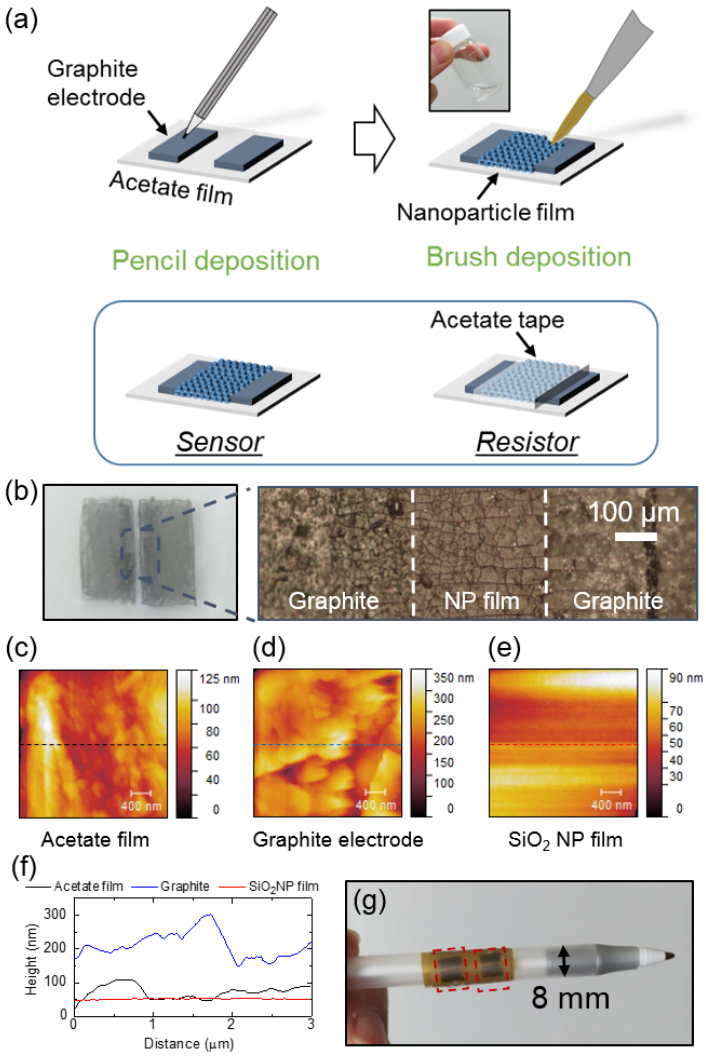

Figure 1. (a) Schematic illustration of fabrication of an all-painted sensor. Inset photo shows a colloidal solution of SiO_2 NPs. (b) Whole picture and optical microscope image of an all-painted film. (c-e) AFM images of (c) acetate film, (d) graphite electrode, and (e) SiO_2 NP film, respectively. (f) Height profiles in (c), (d), and (e). (g) Picture of an all-painted device wrapped around a pen (diameter: 8 mm).

RESULTS AND DISCUSSION

Humidity dependence of all-painted device. A deposited SiO_2 NP film works as a humidity-sensitive film; and thus, the device works as a humidity sensor. Figure 2(a) shows current versus voltage characteristics of an all-painted humidity sensor in various RH. Under <10 % RH, no current larger than base noise (~50 pA) is observed because the SiO_2 NP film is insulator. Current intensity due to proton transport increases as RH increases because water molecular layers are formed on a surface of the NP film[44–46]. Note that current intensity without a NP film is 30 times smaller than that with a NP film at 40 % RH (Figure S2). Resistance of a painted SiO_2 NP film versus RH is shown in Figure 2(b). Resistance changes by four orders of magnitude from 10 to 80 %RH due to proton transport on insulator, which is similar to the case of a drop-coated SiO_2 NP film[16]. The resistance is more than 10 MΩ and much larger than the resistance of the graphite electrodes. A Cole-Cole plot of a NP film at 84 % RH is shown in Figure 2(c). From 100 Hz to 1 MHz, the plot shows a semicircle due to an equivalent parallel circuit of a resistance of a NP film (30 MΩ) and a parasitic capacitance (3.3 pF)[47,48]. On the contrary, a diffusion effect of protons appears in the frequency lower than 100 Hz and the impedance slightly increases as the frequency decreases (Warburg impedance)[38,48,49]. Figure S3(a) shows Bode plots of impedance magnitude. Equivalent circuits in 18 and 84 % RH from impedance spectroscopy are shown in Figure S3(b). In the Supporting Information (Figure S4 (a-d)), the Cole-Cole plots of another NP film in different RH are shown. After exposure to 93 % RH, the current-voltage characteristics do not degrade (Figure S4(e)). Thus, this NP film can be in use for detecting human breath which has almost 100 % RH.

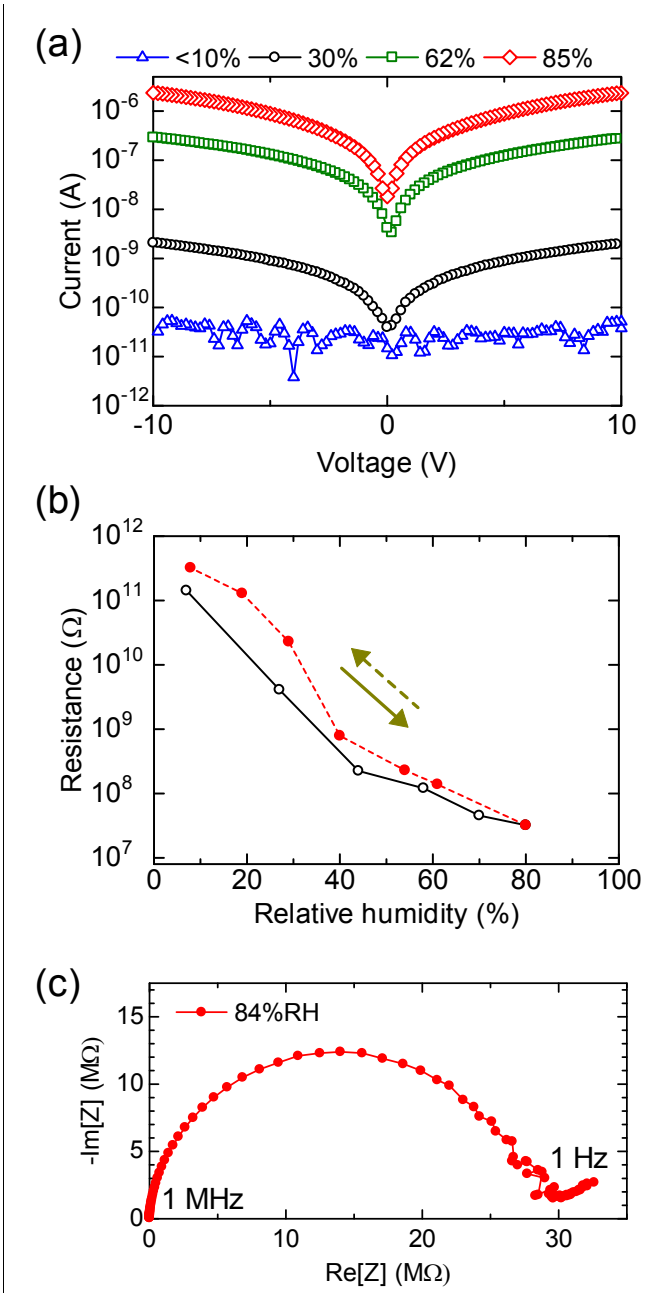

Figure 2. (a) Current versus voltage characteristics of an all-painted humidity sensor in various RH. (b) Resistance of an all-painted humidity sensor as a function of RH. Open and filled marks represent measurements increasing and decreasing humidity, respectively. (c) Cole-Cole plot of a painted SiO_2 NP film. Frequency changes from 1 Hz to 1 MHz. All of the measurements were used in a homemade box.

To prove the concept to fabricate a NP film sensor by all-painting processes, we fabricate 15 humidity sensors as shown in Figure 3(a). All the sensors show similar current-voltage curves (Figure S5(a)). The resistance response to dynamic humidity change between 30 and 84 % RH is shown in Figure 3(b). Figure 3(c) shows the variation of the sensor resistance. The average resistances at 30 % and 84 % RH are 1.4 GΩ and 34 MΩ, respectively. Response time and recovery time are defined as the time to achieve 90% of total change. The response time and recovery time of all-painted sensors are evaluated to be 31.4 and 6.5 s, respectively (Figure S5(b)).

It is noted that the response is sufficient enough to detect human respiration (~0.2 Hz) because we use a dynamic output to humidity change. A current change of 10 % of total change is detectable and the average time to achieve 10 % of total change of current are 4.8 (rise) and 0.7 (fall) s, respectively (Figure S5(c) and (d)). Therefore, we do not need to use a saturated signal of the humidity sensor in this application. It is possible to calculate human breathing rates by counting the number of peaks of the dynamic output as shown later.

A possible method to decrease the response/recovery time is to reduce the thickness of the 400-nm SiO_2 NP film. According to Miao et al.[50], water absorption capacity of a thinner humidity-sensitive film might result in short response/recovery time. Another possible method is to reduce the gap between graphite electrodes. However, it is difficult to prepare a shorter gap than 200 μm by pencil drawing and we cannot examine the gap size dependence. Table 1 shows statistical values of sensor properties. We do not have a clear reason why the recovery time is shorter than the response time.

Table 1. Statistical values of sensor properties

	Resistance in 84 %RH	Resistance in 30 %RH	Rise time	Fall time
Average	34 MΩ	1.4 GΩ	4.8 s	0.7 s
Standard deviation	20 MΩ	0.97 GΩ	1.7 s	0.4 s

We discuss an appropriate substrate for all-painted humidity sensors. We can fabricate an all-painted humidity sensor on a photocopying cellulose paper. However, a painted NP film on a photocopying cellulose paper shows much slower response (response/recovery time: 535/86.8 s, Figure S6). When a colloidal solution is deposited on a photocopying paper, SiO_2 NPs are dispersed inside the paper and the whole paper becomes a humidity-sensitive film. Because water molecules are trapped on SiO_2 NPs inside the paper, response and recovery of the sensor become slow. This result indicates that a substrate for all-painted humidity sensors needs water-resistance and does not absorb colloidal solution.

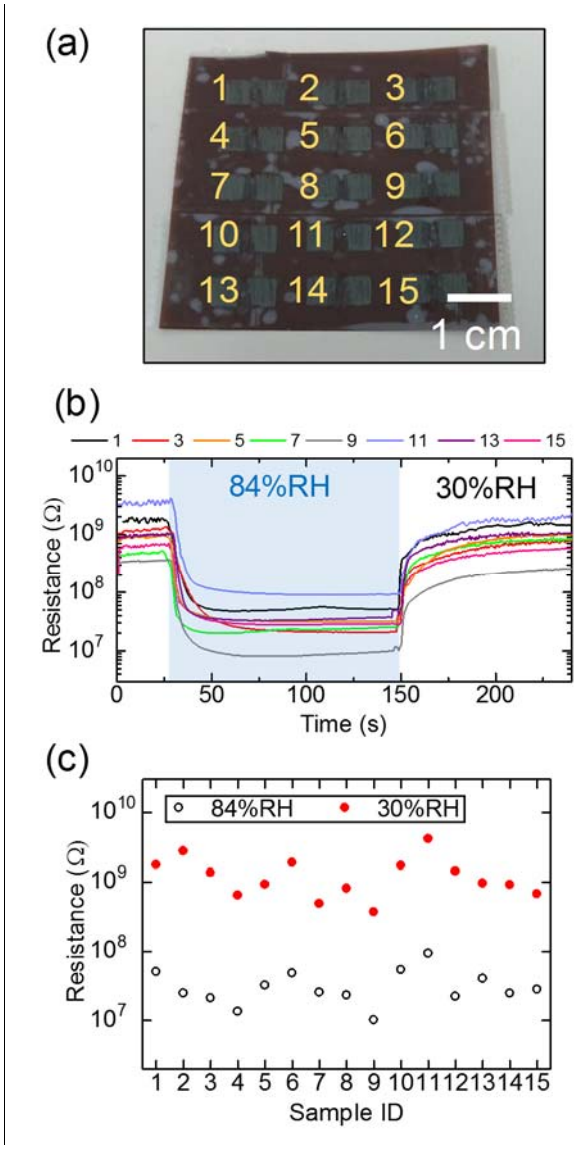

Figure 3. (a) Picture of 15 painted humidity sensors. Sample IDs are shown in the picture. Acetate films are attached on a polyimide film (125 μm thickness). (b) Dynamic response of resistance of painted films by changing humidity. 10 V is applied as a bias voltage. (c) Resistance distribution of painted films in 84 % and 30 % RH.

Bending cycle test. Figure 4(a) shows a resistance of an all-painted NP humidity sensor as a function of bending radius of curvature. Resistance does not largely change even in the radius of curvature (*r*) of 1.3 mm. Fluctuation of the resistance may be due to change of a current path through the bent SiO2 NP film. As the number of bending cycles increases, the resistance increases as shown in Figure 4(b) because the SiO_2 NP film is possibly damaged by bending. However, even after 500 times bending tests in r=1.3 mm, the sensor detects exhaled air from nose (distance from the sensor: ~10 cm). Figure 4(c) and 4(d) show responses of the sensor to exhaled air before and after 500 bending cycles, respectively. Five successive respiration can be detected after the bending cycle test. The fluctuation of the current intensity under exhaled air is due to the fluctuation of human respiration because the amount of exhaled air and the rate are not precisely controlled. The results in Figure 4 indicate that the all-painted SiO_2 NP sensor has high flexibility.

Table 2 summarizes recent literature reporting humidity sensors on cellulose. Despite the simple and easy fabrication process, the sensitivity (10^6 % between 10-93 %RH) and response/recovery time (31.4 s/6.5 s) of the all-painted sensor are as good as those of the previous reported paper-based humidity sensors. Table 2 also includes recent literature on ultrafast response and flexible polymer humidity sensors. Compared to these sensors, an advantage of the all-painted sensor is the easiness of the fabrication process, which does not require any electrical facilities, such as printing and vacuum evaporation facilities. It is beneficial if human respiration is monitored by using the all-painted humidity sensor produced on site.

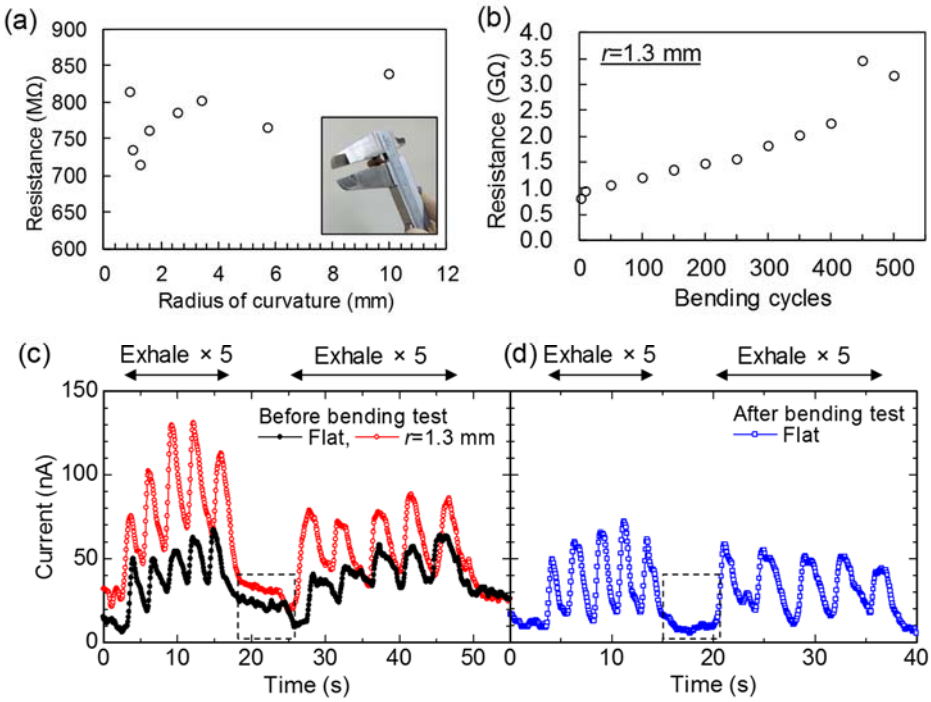

Figure 4. (a-b) Resistance of an all-painted humidity sensor as a function of (a) radius of curvature and (b) bending cycles in r=1.3 mm. (c-d) Response to exhaled air (c) before and (d) after the bending test. Current under bending in r=1.3 mm is also shown in (c). Dashed rectangles indicate that the current intensity under no exhaled air.

Table 2. Properties of humidity sensors on cellulose in recent literature. NA: No data. Properties of ultrafast response and flexible polymer humidity sensors are also shown for comparison.

humidity-sensitive material	electrode	substrate	sensor type	RH range	sensitivity	response time/ recovery time
oxidized MWCNTs[34]	graphite	cellulose	resistance	33-95 %	18-33 %	5-8 min/7-11 min
cellulose[33]	graphite	cellulose	capacitance	30-90 %	230 %	10 s/32 s
CNT[29]	copper foil tape	cellulose	resistance	10-70 %	60 %	6 s/120 s
cellulose[13]	graphite	cellulose	resistance	20-90 %	10^6 %	1500 s/NA
cellulose[31]	silver nanoparticle	cellulose	resistance	20-90 %	10^6 %	NA/NA
SiO_2 NPs (This work)	graphite	cellulose acetate	resistance	10-93 %	10^6 %	31.4 s/6.5 s
graphene oxide[51]	silver	polyethylene naphthalene	resistance	35-80%	10^4 %	30 ms/30 ms
supramolecular nanofiber[52,53]	gold	glass	resistance	5-90 %	10^6 %	8 ms/ 24 ms
silicon nanocrystal film[19]	gold	polyimide	resistance	10-80 %	10^7 %	40 ms/40 ms
polypyrrole/polyoxomethalate[50]	silver	glass	resistance	11-98%	170 %	1.9 s/1.1 s
wrinkled graphene[14]	silver	silicon wafer	resistance	11-95 %	126 % (=1.5 %/1 %RH)	12.5 ms/ 12.5 ms

All-painted resistor with SiO_2 NP film. In order to fabricate a portable respiration sensor, we design an electrical circuit in Figure 5(a). The circuit consists of a humidity sensor (R_R) and a resistor (R_L) which are solely fabricated by painting. A bias voltage from a button buttery is applied to a series of R_R and R_L, and then an output voltage V_{out} in R_L is monitored. The output voltage in Figure 5(a) is changed by large R_R change when R_R is exposed to exhaled air.

It should be stressed here that we also fabricate a resistor (a humidity-insensitive element) by painting. A resistor is fabricated by covering a SiO_2 NP film with an acetate tape (Figure 5(b)). Although the current-voltage curve does not largely change with covering the surface (Figure 5(c)), the resistance becomes independent on humidity as shown in Figure 5(d). This indicates a surface-covered NP film is protected by the tape from adsorption of water molecules. With assembling all-painted resistor and humidity sensor, we can demonstrate an all-painted respiration sensor as follows.

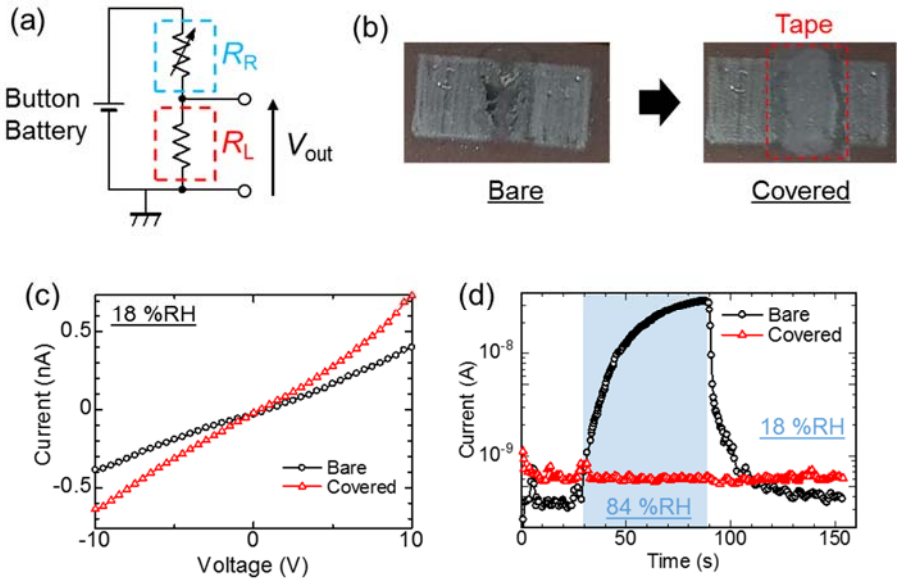

Figure 5. (a) Electrical circuit of an all-painted respiration sensor. R_R and R_L represent a humidity sensor with a bare SiO_2 NP film and a resistor with a surface-covered SiO_2 NP film, respectively. (b) Photos of bare and surface-covered SiO_2 NP films. (c) Current-voltage curves and (d) current response to humidity change of the SiO_2 NP films. Colored region in (d) indicates that the films are in 84 % RH. A bias voltage (10 V) is applied to each device in (d).

Bifunctional monitoring of respiration and exhaled air temperature. Figure 6(a) shows a sensor structure for a portable bifunctional healthcare device. Figure 6(b) shows a sensor response to a finger proximity within 2 mm. Water evaporation from a fingertip is clearly monitored as increase of the output voltage (Figure S7(a) and S7(b)). Figure 6(c) is a picture of an attached healthcare device on a medical oxygen mask. The device is placed near ventilation holes of the oxygen mask. A portable data logger is also attached on a mask with a single-side tape. Figure 6(d) shows response of the healthcare device to three deep respiration of a subject at rest. The device detects respiration and exhaled air temperature (~35 ^{o}C) from the subject (body temperature: ~36 ^{o}C). Exhaled air temperature is lower than body temperature by ~1^{o}C. Humidity in the exhaled breath is almost saturated (~100 %) because breath air is humidified by human respiratory systems. 2.3 V of the response corresponds to 100 % RH in this study. It should be noted that the all-printed respiration sensor can follow various respiration patterns (up to 40 min^{-1}) such as apnea, hyperpnoea, and dyspnea (Figure S7(c)). The sensor signals are clear with high S/N ratio (~23) without baseline drifting.

Figure 6(e) shows respiration and temperature of exhaled air during walk and run. The sensor fully tracks an increase of respiration rate (14 min^{-1} to 20 min^{-1}) by running. Because the output of the temperature sensor clearly corresponds to that of the all-painted NP respiration sensor, we prove the all-painted respiration sensor works correctly. However, the temperature sensor does not fully follow the exhaled air temperature in this measurement because of the slow response. Because graphite and SiO_2 NP are robust and chemically stable, the sensor can be stored in ambient air more than 20 days (Figure S7(d)). The breathing patterns of “Walk”, “Run” and “Rest” in Figure 6(e) is shown in the Supporting Information (Figure S7). The shape of the signals is almost identical. We checked that volatile organic compounds (VOCs) in exhaled gas do not have influence in the sensor output (Figure S9). This portable bifunctional

respiration sensor has a large impact for many fields such as extreme sports, early finding of disease, and physiological evaluation[14,19].

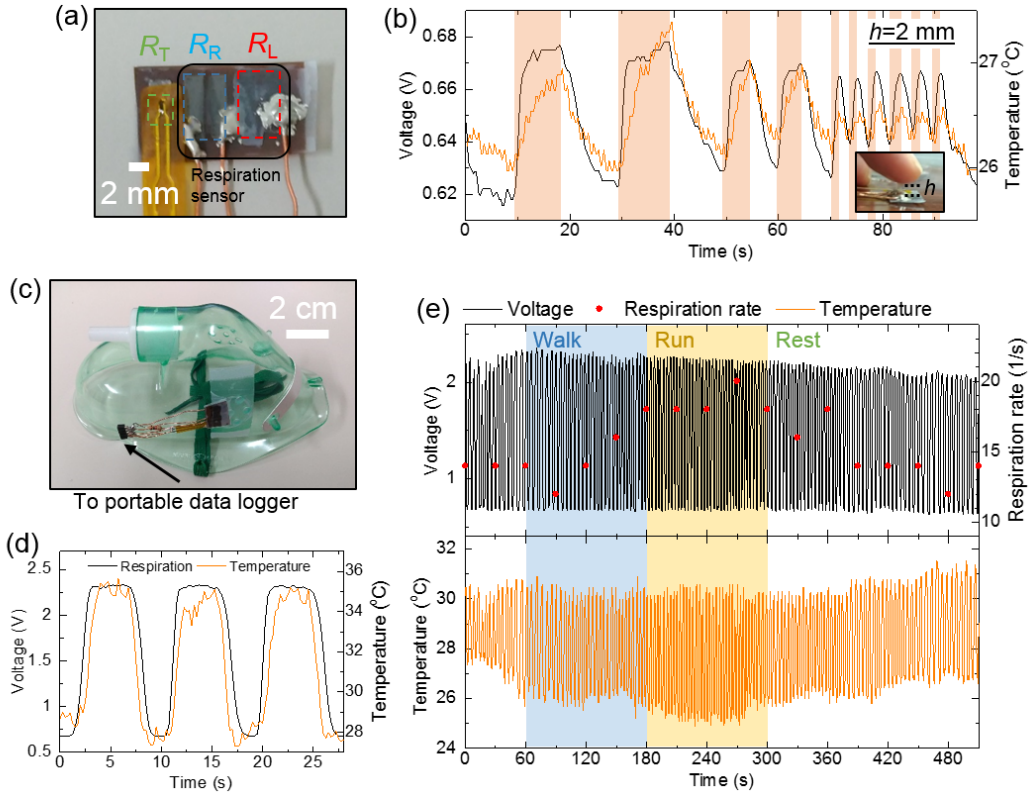

Figure 6. (a) Prototype of a portable healthcare device using an all-painted respiration sensor and a flexible temperature sensor. (b) Response of the device to finger proximity (2 mm away). Shadowed regions correspond to the time in a finger proximity. (c) Attached healthcare device on a medical oxygen mask. (d) Response to deep respiration. (e) Demonstration of successive monitoring of respiration rate and exhaled air temperature in exercise.

CONCLUSIONS

We have developed an all-painting process to produce a sensitive respiration sensor by using solely hand-painting. The sensor was prepared with a brush-painted humidity-sensitive NP film and graphite traces, which were low-cost and non-toxic green materials. We first demonstrated an all-painted humidity sensor on an acetate film. Reproducible fabrication was achieved and the sensitivity and the response/recovery time of the humidity sensor were 10^4 and 31.4 s/6.5 s, respectively. The humidity sensor was flexible and operated normally after 500 bending cycles in r=1.3 mm. We designed an all-painted respiration sensor comprising the humidity sensor and a painted resistor. We integrated the all-painted respiration sensor, a thermistor, and a portable data logger as a portable bifunctional healthcare device. The healthcare device simultaneously tracked human respiration rate and exhaled air temperature. Painting is a simple, easy, and green process to produce healthcare devices for social demands without electrical facilities.

ASSOCIATED CONTENT

Supporting information

The Supporting Information is available free of charge on the ACS Publications website at DOI:***. AFM images, profiles, and a SEM image of a SiO_2 NP film; Current-voltage curves of graphite electrodes without a NP film; Bode plots of a NP film; Cole-Cole plots in different relative humidity; Characteristics of 15 all-painted sensors; Characteristics of all-painted sensor on a photocopying paper; Detection of water evaporation from a fingertip and various rates of respiration patterns; each breathing pattern of Figure 6(e); VOC gas exposure test.

AUTHOR INFORMATION

Corresponding Author

*E-mail: kano@eedept.kobe-u.ac.jp (S.K)

Notes

The authors declare no competing financial interest. The research has been approved by the institutional review board in Kobe University.

ACKNOWLEDGMENTS

This work was partly supported by JSPS KAKENHI Grant Number 16H03828 and 18K13767, and Visegrad Group (V4)-Japan Joint Research Project on Advanced Materials “NaMSeN”.

REFERENCES

(1) Khan, Y.; Ostfeld, A. E.; Lochner, C. M.; Pierre, A.; Arias, A. C. Monitoring of Vital Signs with Flexible and Wearable Medical Devices. *Adv. Mater.* **2016**, *28* (22), 4373–4395, DOI: 10.1002/adma.201504366.

(2) Trung, T. Q.; Lee, N. E. Flexible and Stretchable Physical Sensor Integrated Platforms for Wearable Human-Activity Monitoring and Personal Healthcare. *Adv. Mater.* **2016**, *28* (22), 4338–4372, DOI: 10.1002/adma.201504244.

(3) Yao, S.; Swetha, P.; Zhu, Y. Nanomaterial-Enabled Wearable Sensors for Healthcare. *Adv. Healthc. Mater.* **2018**, *7* (1), 1–27, DOI: 10.1002/adhm.201700889.

(4) El-Amrawy, F.; Nounou, M. I. Are Currently Available Wearable Devices for Activity Tracking and Heart Rate Monitoring Accurate, Precise, and Medically Beneficial? *Healthc. Inform. Res.* **2015**, *21* (4), 315–320, DOI: 10.4258/hir.2015.21.4.315.

(5) Bandodkar, A. J.; Jeerapan, I.; Wang, J. Wearable Chemical Sensors: Present Challenges and Future Prospects. *ACS Sensors* **2016**, acssensors.6b00250, DOI: 10.1021/acssensors.6b00250.

(6) Ho, D. H.; Sun, Q.; Kim, S. Y.; Han, J. T.; Kim, D. H.; Cho, J. H. Stretchable and Multimodal All Graphene Electronic Skin. *Adv. Mater.* **2016**, *28* (13), 2601–2608, DOI: 10.1002/adma.201505739.

(7) Harada, S.; Honda, W.; Arie, T.; Akita, S.; Takei, K. Fully Printed, Highly Sensitive Multifunctional Artificial Electronic Whisker Arrays Integrated with Strain and Temperature Sensors. *ACS Nano* **2014**, *8* (4), 3921–3927, DOI: 10.1021/nn500845a.

(8) Yamamoto, Y.; Harada, S.; Yamamoto, D.; Honda, W.; Arie, T.; Akita, S.; Takei, K. Printed Multifunctional Flexible Device with an Integrated Motion Sensor for Health Care Monitoring. *Sci. Adv.* **2016**, *2* (11), e1601473–e1601473, DOI: 10.1126/sciadv.1601473.

(9) Xu, H.; Xiang, J. X.; Lu, Y. F.; Zhang, M. K.; Li, J. J.; Gao, B. B.; Zhao, Y. J.; Gu, Z. Z. Multifunctional Wearable Sensing Devices Based on Functionalized Graphene Films for Simultaneous Monitoring of Physiological Signals and Volatile Organic Compound Biomarkers. *ACS Appl. Mater. Interfaces* **2018**, *10* (14), 11785–11793, DOI: 10.1021/acsami.8b00073.

(10) Atalay, O.; Kennon, W. R.; Demirok, E. Weft-Knitted Strain Sensor for Monitoring Respiratory Rate and Its Electro-Mechanical Modeling. *IEEE Sens. J.* **2015**, *15* (1), 110–122, DOI: 10.1109/JSEN.2014.2339739.

(11) Atalay, O.; Atalay, A.; Gafford, J.; Wang, H.; Wood, R.; Walsh, C. A Highly Stretchable Capacitive-Based Strain Sensor Based on Metal Deposition and Laser Rastering. *Adv. Mater. Technol.* **2017**, *1700081*, 1–8, DOI: 10.1002/admt.201700081.

(12) Kundu, S. K.; Kumagai, S.; Sasaki, M. A Wearable Capacitive Sensor for Monitoring Human Respiratory Rate. *Jpn. J. Appl. Phys.* **2013**, *52* (4S), 04CL05, DOI: 10.7567/JJAP.52.04CL05.

(13) Güder, F.; Ainla, A.; Redston, J.; Mosadegh, B.; Glavan, A.; Martin, T. J.; Whitesides, G. M. Paper-Based Electrical Respiration Sensor. *Angew. Chemie - Int. Ed.* **2016**, *55* (19), 5727–5732, DOI: 10.1002/anie.201511805.

(14) Zhen, Z.; Li, Z.; Zhao, X.; Zhong, Y.; Zhang, L.; Chen, Q.; Yang, T.; Zhu, H. Formation of Uniform Water Microdroplets on Wrinkled Graphene for Ultrafast Humidity Sensing. *Small* **2018**, *1703848*, 1–8, DOI: 10.1002/smll.201703848.

(15) Kim, Y.; Lu, J.; Shih, B.; Gharibans, A.; Zou, Z.; Matsuno, K.; Aguilera, R.; Han, Y.; Meek, A.; Xiao, J.; et al. Scalable Manufacturing of Solderable and Stretchable Physiologic Sensing Systems. *Adv. Mater.* **2017**, *1701312*, 1–11, DOI: 10.1002/adma.201701312.

(16) Kano, S.; Dobashi, Y.; Fujii, M. Silica Nanoparticle-Based Portable Respiration Sensor for Analysis of Respiration Rate, Pattern, and Phase During Exercise. *IEEE Sensors Lett.* **2018**, *2* (1), 1–4, DOI: 10.1109/LSENS.2017.2787099.

(17) Kano, S.; Fujii, M. Battery-Powered Wearable Respiration Sensor Chip with Nanocrystal Thin Film. In *2017 IEEE SENSORS*; IEEE, 2017; pp 1293–1295, DOI: 10.1109/ICSENS.2017.8234307.

(18) Segev-bar, M.; Haick, H. Flexible Sensors Based on Nanoparticles. *ACS Nano* **2013**, *7* (10), 8366–8378, DOI: 10.1021/nn402728g.

(19) Kano, S.; Kim, K.; Fujii, M. Fast-Response and Flexible Nanocrystal-Based Humidity Sensor for Monitoring Human Respiration and Water Evaporation on Skin. *ACS Sensors* **2017**, *2*, 828–833, DOI: 10.1021/acssensors.7b00199.

(20) Mahadeva, S. K.; Walus, K.; Stoeber, B. Paper as a Platform for Sensing Applications and Other Devices: A Review. *ACS Appl. Mater. Interfaces* **2015**, *7* (16), 8345–8362, DOI: 10.1021/acsami.5b00373.

(21) Kurra, N.; Kulkarni, G. U. Pencil-on-Paper: Electronic Devices. *Lab Chip* **2013**, *13* (15), 2866, DOI: 10.1039/c3lc50406a.

(22) Irimia-Vladu, M. "Green" Electronics: Biodegradable and Biocompatible Materials and Devices for Sustainable Future. *Chem. Soc. Rev.* **2014**, *43* (2), 588–610, DOI: 10.1039/C3CS60235D.

(23) Fortunato, E.; Correia, N.; Barquinha, P.; Pereira, L.; Gonçalves, G.; Martins, R. High-Performance Flexible Hybrid Field-Effect Transistors Based on Cellulose Fiber Paper. *Electron Device Lett. IEEE* **2008**, *29* (9), 988–990, DOI: 10.1109/LED.2008.2001549.

(24) Kurra, N.; Dutta, D.; Kulkarni, G. U. Field Effect Transistors and RC Filters from Pencil-Trace on Paper. *Phys. Chem. Chem. Phys.* **2013**, *15* (21), 8367, DOI: 10.1039/c3cp50675d.

(25) Mazzeo, A. D.; Kalb, W. B.; Chan, L.; Killian, M. G.; Bloch, J. F.; Mazzeo, B. A.; Whitesides, G. M. Paper-Based, Capacitive Touch Pads. *Adv. Mater.* **2012**, *24* (21), 2850–2856, DOI: 10.1002/adma.201200137.

(26) Nagashima, K.; Koga, H.; Celano, U.; Zhuge, F.; Kanai, M.; Rahong, S.; Meng, G.; He, Y.; De Boeck, J.; Jurczak, M.; et al. Cellulose Nanofiber Paper as an Ultra Flexible Nonvolatile Memory. *Sci. Rep.* **2014**, *4*, 5532, DOI: 10.1038/srep05532.

(27) Lien, D. H.; Kao, Z. K.; Huang, T. H.; Liao, Y. C.; Lee, S. C.; He, J. H. All-Printed Paper Memory. *ACS Nano* **2014**, *8* (8), 7613–7619, DOI: 10.1021/nn501231z.

(28) Lin, C. W.; Zhao, Z.; Kim, J.; Huang, J. Pencil Drawn Strain Gauges and Chemiresistors on Paper. *Sci. Rep.* **2014**, *4*, 1–6, DOI: 10.1038/srep03812.

(29) Han, J. W.; Kim, B.; Li, J.; Meyyappan, M. Carbon Nanotube Based Humidity Sensor on Cellulose Paper. *J. Phys. Chem. C* **2012**, *116* (41), 22094–22097, DOI: 10.1021/jp3080223.

(30) Mahadeva, S. K.; Yun, S.; Kim, J. Flexible Humidity and Temperature Sensor Based on Cellulose-Polypyrrole Nanocomposite. *Sensors Actuators, A Phys.* **2011**, *165* (2), 194–199, DOI: 10.1016/j.sna.2010.10.018.

(31) Barmpakos, D.; Segkos, A.; Tsamis, C.; Kaltsas, G. A Disposable Flexible Humidity Sensor Directly Printed on Paper for Medical Applications. *J. Phys. Conf. Ser.* **2017**, *931* (1), DOI: 10.1088/1742-6596/931/1/012003.

(32) Jung, M.; Kim, K.; Kim, B.; Cheong, H.; Shin, K.; Kwon, O. S.; Park, J. J.; Jeon, S. Paper-Based Bimodal Sensor for Electronic Skin Applications. *ACS Appl. Mater. Interfaces* **2017**, *9* (32), 26974–26982, DOI: 10.1021/acsami.7b05672.

(33) Kanaparthi, S. Pencil-Drawn Paper-Based Non-Invasive and Wearable Capacitive Respiration Sensor. *Electroanalysis* **2017**, *29* (12), 2680–2684, DOI: 10.1002/elan.201700438.

(34) Zhao, H.; Zhang, T.; Qi, R.; Dai, J.; Liu, S.; Fei, T. Drawn on Paper: A Reproducible Humidity Sensitive Device by Handwriting. *ACS Appl. Mater. Interfaces* **2017**, *9* (33), 28002–28009, DOI: 10.1021/acsami.7b05181.

(35) Zhang, Y.; Duan, Z.; Zou, H.; Ma, M. Drawn a Facile Sensor: A Fast Response Humidity Sensor Based on Pencil-Trace. *Sensors Actuators, B Chem.* **2018**, *261*, 345–353, DOI: 10.1016/j.snb.2018.01.176.

(36) Noh, Y. Y.; Zhao, N.; Caironi, M.; Sirringhaus, H. Downscaling of Self-Aligned, All-Printed Polymer Thin-Film Transistors. *Nat. Nanotechnol.* **2007**, *2* (12), 784–789, DOI: 10.1038/nnano.2007.365.

(37) Bandodkar, A. J.; Nuñez-Flores, R.; Jia, W.; Wang, J. All-Printed Stretchable Electrochemical Devices. *Adv. Mater.* **2015**, *27* (19), 3060–3065, DOI: 10.1002/adma.201500768.

(38) Zhao, H.; Zhang, T.; Qi, R.; Dai, J.; Liu, S.; Fei, T.; Lu, G. Humidity Sensor Based on Solution Processible Microporous Silica Nanoparticles. *Sensors Actuators, B Chem.* **2018**, *266*, 131–138, DOI: 10.1016/j.snb.2018.03.052.

(39) Wang, C.-T.; Wu, C.-L.; Chen, I.-C.; Huang, Y.-H. Humidity Sensors Based on Silica Nanoparticle Aerogel Thin Films. *Sensors Actuators B Chem.* **2005**, *107* (1), 402–410, DOI: 10.1016/j.snb.2004.10.034.

(40) Boles, M. A.; Engel, M.; Talapin, D. V. Self-Assembly of Colloidal Nanocrystals: From Intricate Structures to Functional Materials. *Chem. Rev.* **2016**, *116* (18), 11220–11289, DOI: 10.1021/acs.chemrev.6b00196.

(41) Zhang, D.; Tong, J.; Xia, B.; Xue, Q. Ultrahigh Performance Humidity Sensor Based on Layer-by-Layer Self-Assembly of Graphene Oxide/Polyelectrolyte Nanocomposite Film. *Sensors Actuators, B Chem.* **2014**, *203*, 263–270, DOI: 10.1016/j.snb.2014.06.116.

(42) Yan, H.; Zhang, L.; Yu, P.; Mao, L. Sensitive and Fast Humidity Sensor Based on A Redox Conducting Supramolecular Ionic Material for Respiration Monitoring. *Anal. Chem.* **2017**, *89* (1), 996–1001, DOI: 10.1021/acs.analchem.6b04350.

(43) Popov, T. A.; Kralimarkova, T. Z.; Dimitrov, V. D. Measurement of Exhaled Breath Temperature in Science and Clinical Practice. *Breathe* **2012**, *8* (3), 186–192, DOI: 10.1183/20734735.021811.

(44) Agmon, N. The Grotthuss Mechanism. *Chem. Phys. Lett.* **1995**, *244* (5–6), 456–462, DOI: 10.1016/0009-2614(95)00905-J.

(45) Chen, Z.; Lu, C. Humidity Sensors: A Review of Materials and Mechanisms. *Sens. Lett.* **2005**, *3* (4), 274–295, DOI: 10.1166/sl.2005.045.

(46) Sasaki, M.; Kano, S.; Sugimoto, H.; Imakita, K.; Fujii, M. Surface Structure and Current Transport Property of Boron and Phosphorous Co-Doped Silicon Nanocrystals. *J. Phys. Chem. C* **2016**, *120* (1), 195–200, DOI: 10.1021/acs.jpcc.5b05604.

(47) Kano, S.; Sasaki, M.; Fujii, M. Combined Analysis of Energy Band Diagram and Equivalent Circuit on Nanocrystal Solid. *J. Appl. Phys.* **2016**, *119* (21), 215304, DOI: 10.1063/1.4953216.

(48) Jiang, K.; Zhao, H.; Dai, J.; Kuang, D.; Fei, T.; Zhang, T. Excellent Humidity Sensor Based on LiCl Loaded Hierarchically Porous Polymeric Microspheres. *ACS Appl. Mater. Interfaces* **2016**, *8* (38), 25529–25534, DOI: 10.1021/acsami.6b08071.

(49) Feng, C.-D.; Sun, S.-L.; Wang, H.; Segre, C. U.; Stetter, J. R. Humidity Sensing Properties of Nation and Sol-Gel Derived SiO2/Nafion Composite Thin Films. *Sensors Actuators B Chem.* **1997**, *40* (2–3), 217–222, DOI: 10.1016/S0925-4005(97)80265-1.

(50) Miao, J.; Chen, Y.; Li, Y.; Cheng, J.; Wu, Q.; Ng, K. W.; Cheng, X.; Chen, R.; Cheng, C.; Tang, Z. Proton Conducting Polyoxometalate/Polypyrrole Films and Their

Humidity Sensing Performance. *ACS Appl. Nano Mater.* **2018**, *1* (2), 564–571, DOI: 10.1021/acsanm.7b00072.

(51) Borini, S.; White, R.; Wei, D.; Astley, M.; Haque, S.; Spigone, E.; Harris, N.; Kivioja, J.; Ryhänen, T. Ultrafast Graphene Oxide Humidity Sensors. *ACS Nano* **2013**, *7* (12), 11166–11173, DOI: 10.1021/nn404889b.

(52) Mogera, U.; Sagade, A. A.; George, S. J.; Kulkarni, G. U. Ultrafast Response Humidity Sensor Using Supramolecular Nanofibre and Its Application in Monitoring Breath Humidity and Flow. *Sci. Rep.* **2014**, *4*, 4103, DOI: 10.1038/srep04103.

(53) Mogera, U.; Gedda, M.; George, S. J.; Kulkarni, G. U. A Supramolecular Nanofiber-Based Passive Memory Device for Remembering Past Humidity. *ACS Appl. Mater. Interfaces* **2017**, *9* (37), 32065–32070, DOI: 10.1021/acsami.7b10732.

Table of Contents Graphics

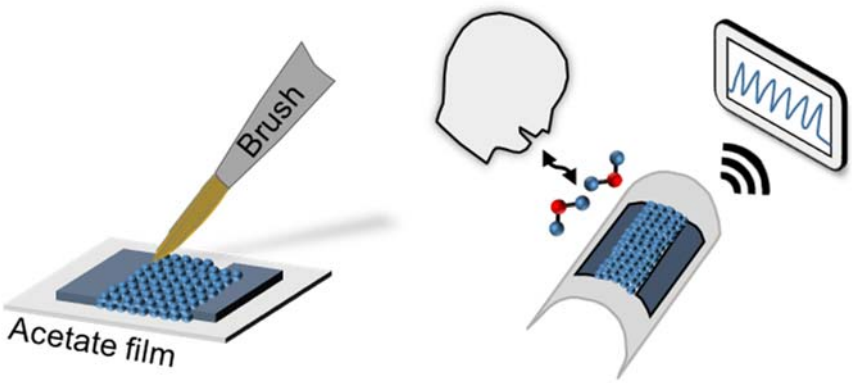

SYNOPSIS: We propose an all-painted fabrication process of a respiration sensor based on a humidity-sensitive silica nanoparticle film and graphite trace.